Supporting Information for

Amino & Triazole-Containing Metal-organic Framework for Highly Efficient CO₂ Fixation

Yang Li,[a] Xueqin Tian,[a] Weiwei Jiang,[a] Pengyan Wu,*[a] Han-Shu Li,[a] Man Wang,[a] Chen Lin[a] and Jian Wang*[a]

[a]School of Chemistry and Materials Science& Jiangsu Key Laboratory of Green Synthetic Chemistry for Functional Materials, Jiangsu Normal University, Xuzhou, 221116, P. R. China.

E-mail: wpyan@jsnu.edu.cn (P.Y. Wu); wjian@jsnu.edu.cn (J. Wang)

Materials and Methods

Reagents and chemicals: All reagents and solvents were of AR grade and used without further purification unless otherwise noted. 4,4',4"-nitrilotribenzoic acid was synthesized according to the literature methods.[S1] 3,5-di(pyridin-4-yl)-4H-1,2,4-triazol-4-amine (dpta) was purchased from Jinan Henghua Technology Co., Ltd. $Zn(NO_3)_2 \cdot 6H_2O$ was purchased from Shanghai Fourth Chemical Reagent Company (China). All of the epoxides (allyl glycidyl ether, butyl glycidyl ether, glycol diglycidyl ether, 2-(phenoxymethyl)oxirane, 2-((4-nitrophenoxy)methyl)oxirane, 2-((4-methoxyphenoxy)methyl)oxirane, 1,3-bis(oxiran-2-ylmethoxy)benzene, bis(4-(oxiran-2-ylmethoxy)phenyl)methane) and Tetrabutylammonium Bromide (TBABr) were purchased from Beijing Innochem Science & Technology Co., Ltd.

Instruments and spectroscopic measurements: The elemental analyses of C, H and N were performed on a Vario EL III elemental analyzer. ^1H NMR spectra were measured on a Bruker-400 spectrometer with Me_4Si as an internal standard. X-Ray powder diffraction (XRD) patterns of the Zn−TDA was recorded on a Rigaku D/max-2400 X−ray powder diffractometer (Japan) using Cu-$K\alpha$ (λ = 1.5405 Å) radiation. FT−IR spectra were recorded as KBr pellets on JASCO FT/IR−430. Thermogravimetric analysis (TGA) was carried out at a ramp rate of 5 °C/min in a nitrogen flow with a Rigaku Thermo plus TG-8120 instrument. The morphologies of the prepared samples were recorded by a Field Emission Scanning Electron Microscopy (SEM) of Hitachi SU8010. Samples were treated *via* Pt sputtering for 90 s before observation. The contents of metal ions were measured by inductively coupled plasma mass spectrometry (ICP-MS; Leeman PROFILE SPEC). The interaction between Zn−TDA and 2-(phenoxymethyl)oxirane molecule was calculated using density functional theory (DFT) method with periodic boundary conditions as implemented in the Vienna Ab initio Simulation Package (VASP 5.4.1). Gas adsorption isotherms were obtained on a BELSORP-max adsorption instrument (BEL Japan Inc.) using a volumetric technique. The initial outgassing of the sample was carried out under high vacuum (P

< 10^{-2} Pa, T = 120 °C) for 24 h to remove solvated water molecules. The CO_2 adsorption isotherms for desolvated compounds were collected in a relative pressure range from 10 to 1.0×10^5 Pa.

BET area calculation：Once a CO_2 monolayer loading is estimated by applying the BET theory to the simulated CO_2 isotherms at 195 K in the relative pressure range of $p/p_0 = 0.05-0.25$, it is converted to a BET area. For this conversion we use:

$$BET\ area = N_m \ \times \ (V_m)_{STP} \ \times N_A \ \times \ S_{CO2}$$

where N_m is the monolayer loading in "m^3(STP)/$g_{adsorbent}$" units, $(V_m)_{STP}$ is the molar density of nitrogen at standard temperature and pressure (33.7 mol/m^3), N_A is the Avogadro number (6.02×10^{23}) and S_{CO2} is the effective cross-sectional area of CO_2 (1.7×10^{-19} m^2).

Experimental

Synthesis of Zn–TDA: 4,4',4"-nitrilotribenzoic acid (H$_3$tca) (3.8 mg, 10 mM), 3,5-di(pyridin-4-yl)-4H-1,2,4-triazol-4-amine (dpta) (4.0 mg, 17 mM), and Zn(NO$_3$)$_2$·6H$_2$O (10 mg, 34 mM) were dissolved in N,N-Dimethylacetamide/water (2/1, 1 mL) in a screw-capped vial. The resulting mixture was placed in an oven at 90°C for 3 days; upon cooling, light yellow block crystals were collected by filtration. Yield: 73%. Anal calc. for [Zn$_3$(tca)$_2$(dpta)]·(DMA)$_3$(H$_2$O): C 54.28, H 4.21, N 10.55%; Found: C 54.19, H 4.19, N 10.52%.

Typical Procedure for the Reaction of CO_2 Cycloaddition of Epoxides: The catalytic reaction was conducted in a 30-mL autoclave reactor, which was purged with 1-MPa CO_2 under constant pressure for 15 min to allow the system equilibration. The vessel was set in an oil bath with frequent stirring at 373 K for 1.5 h. At the end of the reaction, the reactor was opened after placing it in an ice bath for 20 min. The catalysts were separated through centrifugation, and a small aliquot of the supernatant reaction mixture was analyzed by ^{1}H NMR to calculate the reaction yields.

Crystallography:

Intensities were collected on a Bruker SMART APEX CCD diffractometer with graphite monochromated Mo-Kα (λ = 0.71073 Å) using the SMART and SAINT programs. The structure was solved by direct methods and refined on F2 by full-matrix least-squares methods with SHELXTL version 5.1. Non-hydrogen atoms of the ligand backbones were refined anisotropically. Hydrogen atoms within the ligand backbones were fixed geometrically at calculated positions and allowed to ride on the parent non-hydrogen atoms, and the data were treated with the SQUEEZE routine within PLATON.

Crystal data of Zn−TDA: $C_{62}H_{52}N_{10}O_{15}Zn_3$, Mr = 1373.24, Triclinic, space group P-1, a = 13.7019(13), b = 13.9995(12), c = 21.143(2) Å, α = 74.258(5), β = 79.162(5), γ = 63.495(4), V = 3482.6(6) $Å^3$, Z = 2, Dc = 1.310 g cm^{-3}, μ(Mo-Kα) = 1.092 mm^{-1}, T = 296(2) K. 8884 unique reflections [R_{int} = 0.0511]. Final R_I[with $I > 2\sigma(I)$] = 0.0443, wR_2(all data) = 0.1276, GOOF = 1.026. CCDC number: 2094908.

Table S1 Selective bond distance (Å) and angle (°) in Zn−TDA.

Zn(1)–O(5A)	1.968(3)	Zn(1)–O(2)	1.994(2)
Zn(1)–O(1B)	1.998(2)	Zn(1)–N(3)	2.059(3)
Zn(1)–O(3A)	2.418(3)	Zn(2)–O(12C)	1.918(2)
Zn(2)–O(4B)	1.930(2)	Zn(2)–O(6)	1.956(2)
Zn(2)–O(7D)	1.955(2)	Zn(3)–O(9)	1.963(2)
Zn(3)–O(10E)	1.974(3)	Zn(3)–O(8F)	1.978(2)
Zn(3)–N(4)	2.029(3)	Zn(3)–O(11E)	2.297(3)
O(5A)–Zn(1)–O(2)	143.55(12)	O(5A)–Zn(1)–O(1B)	97.44(12)
O(2)–Zn(1)–O(1B)	107.44(11)	O(5A)–Zn(1)–N(3)	100.92(12)
O(2)–Zn(1)–N(3)	102.43(11)	O(1B)–Zn(1)–N(3)	96.04(11)
O(5A)–Zn(1)–O(3A)	58.72(11)	O(2)–Zn(1)–O(3A)	92.65(11)
O(1B)–Zn(1)–O(3A)	155.91(12)	N(3)–Zn(1)–O(3A)	92.35(12)
O(12C)–Zn(2)–O(4B)	117.10(12)	O(12C)–Zn(2)–O(6)	98.40(11)
O(4B)–Zn(2)–O(6)	114.71(10)	O(12C)–Zn(2)–O(7D)	120.45(11)
O(4B)–Zn(2)–O(7D)	103.11(10)	O(7D)–Zn(2)–O(6)	102.57(10)
O(9)–Zn(3)–O(10E)	99.20(11)	O(9)–Zn(3)–O(8F)	101.57(10)
O(10E)–Zn(3)–O(8F)	143.76(12)	O(9)–Zn(3)–N(4)	103.67(11)
O(10E)–Zn(3)–N(4)	106.88(12)	O(8F)–Zn(3)–N(4)	96.64(10)
O(9)–Zn(3)–O(11E)	152.86(13)	O(10E)–Zn(3)–O(11E)	58.90(11)
O(8F)–Zn(3)–O(11E)	91.13(10)	N(4)–Zn(3)–O(11E)	98.48(13)

Symmetry code A: x, 1+y, z; B: 1+x, y, z; C: x, y, -1+z; D: x, -1+y, -1+z; E: 1+x, -1+y, z; F: x, -1+y, z.

Figure S1. Three-dimensionally connected channels in Zn−TDA with the Connolly surfaces (Connolly radius: 1.6 Å) along *a*-axis. Water and DMA molecules are omitted for clarity. The orange arrows indicate the free Lewis acid zinc centers.
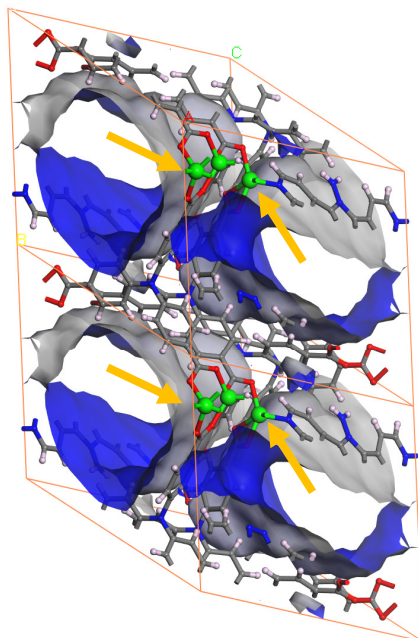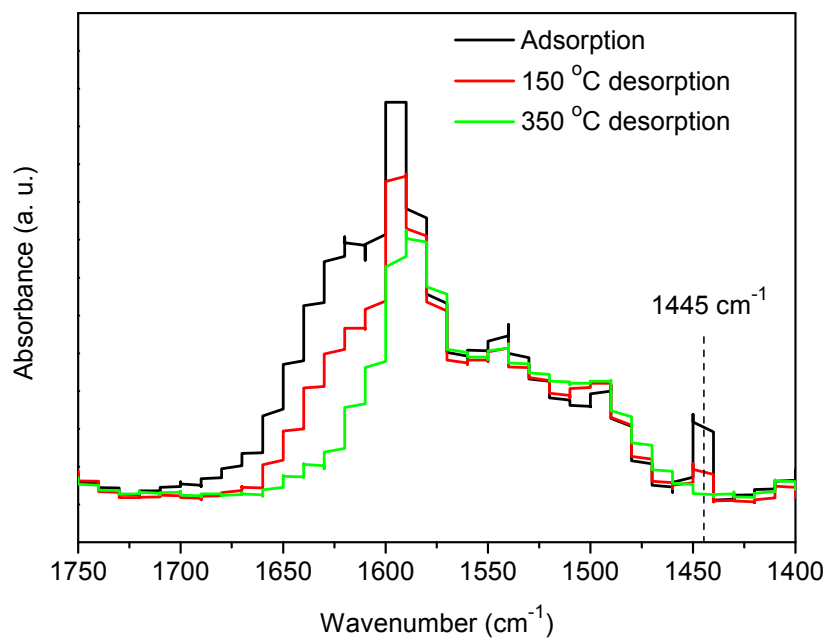
Figure S2. Py-FTIR spectra of Zn−TDA.

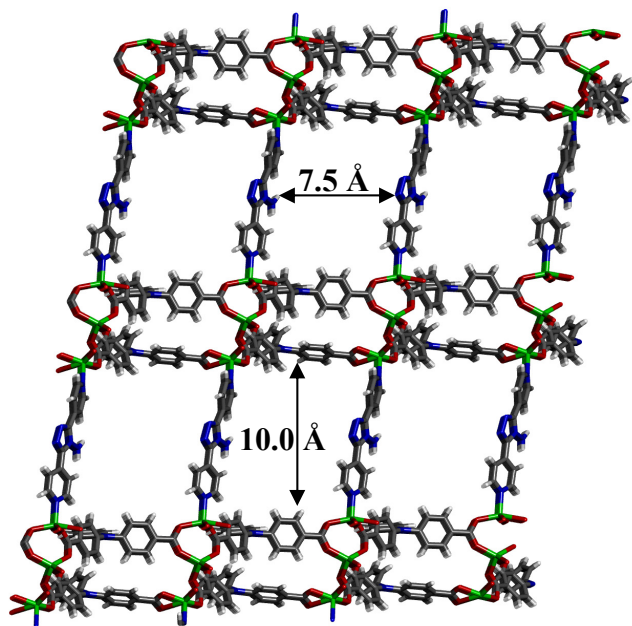**Figure S3**. One-dimensional rectangle channels along the *a*-axis in an identical net of Zn−TDA.
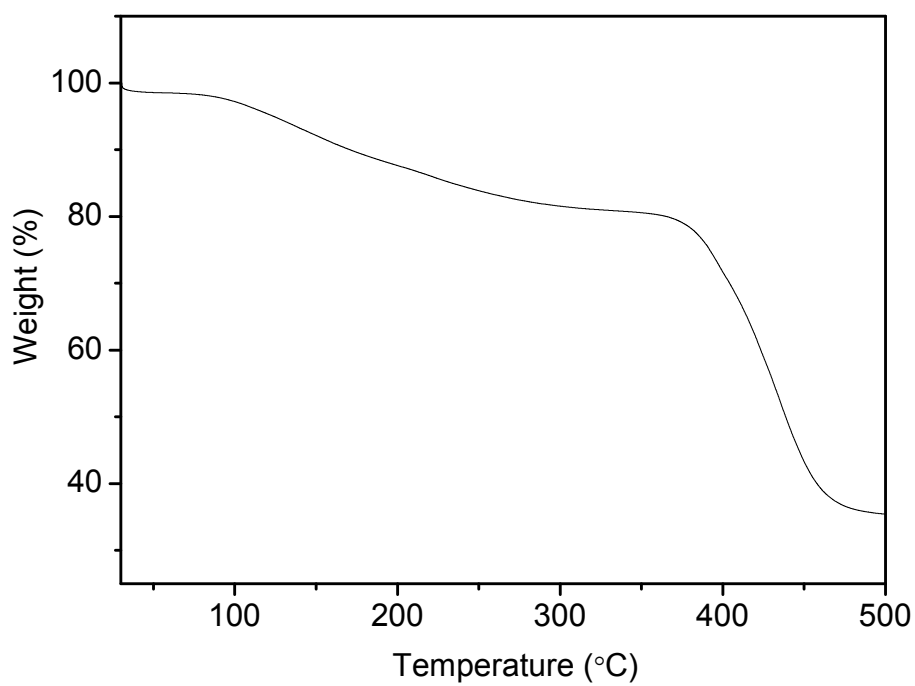
Figure S4. TGA trace of Zn−TDA.

Figure S5. The CO$_2$ isotherms at 273 K and 293 K (symbols) and the virial equation fits (lines) for Zn−TDA.

R^2=0.99964
a_0=-2613.34705
a_1=-40.72815
a_2=1.01029
a_3=-0.00102
a_4=-4.0547E-6
b_0=10.92767
b_1=0.18083
b_2=-0.0042
b_3=9.3177E-6

■ 273 K
● 293 K

InP (torr)

CO$_2$ uptake (mg/g)
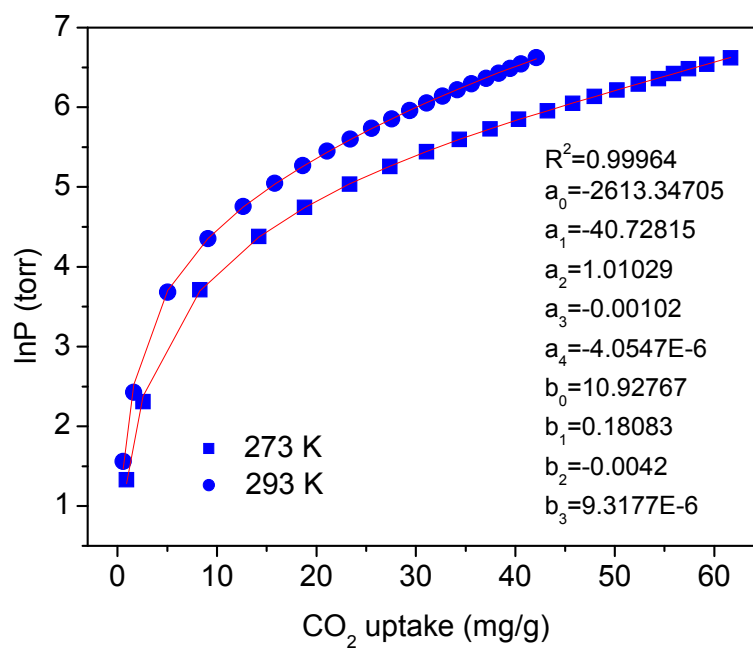
Figure S6. Interaction representation between 2-(phenoxymethyl)oxirane and Zn−TDA computed by density functional theory calculation.
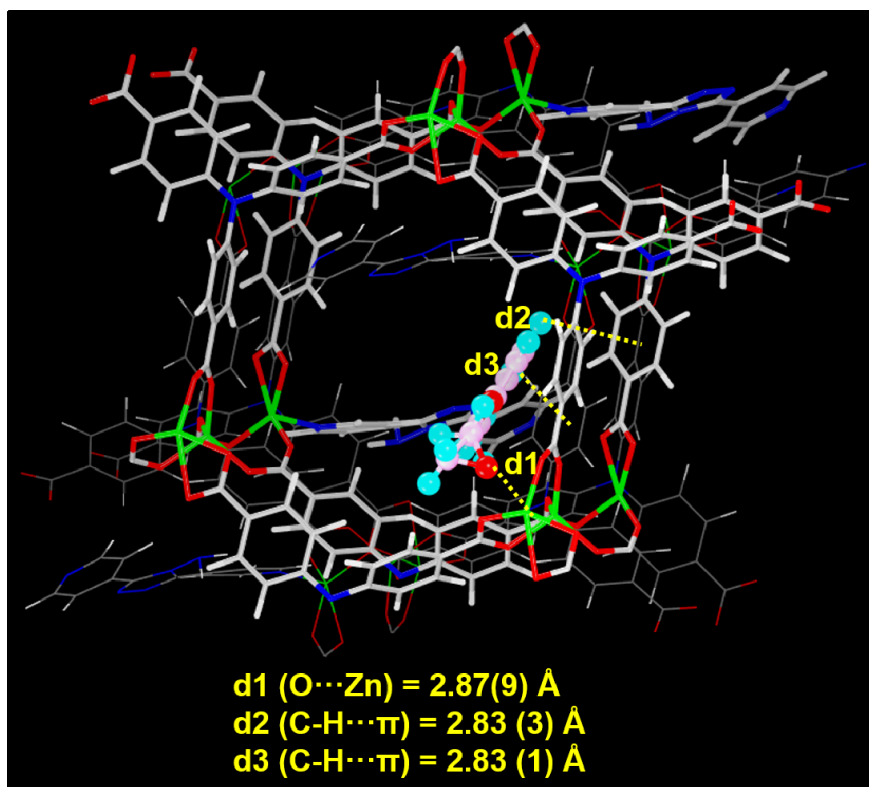
Figure S7. The proposed mechanism for the cycloaddition reaction catalyzed by Zn−TDA (cyan sphere: open metal site).
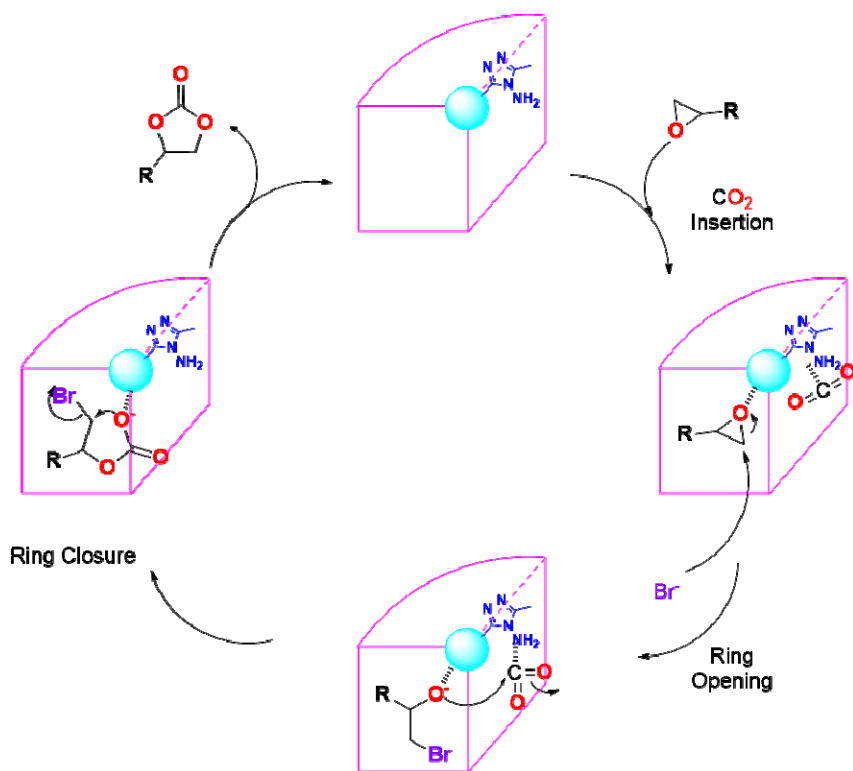
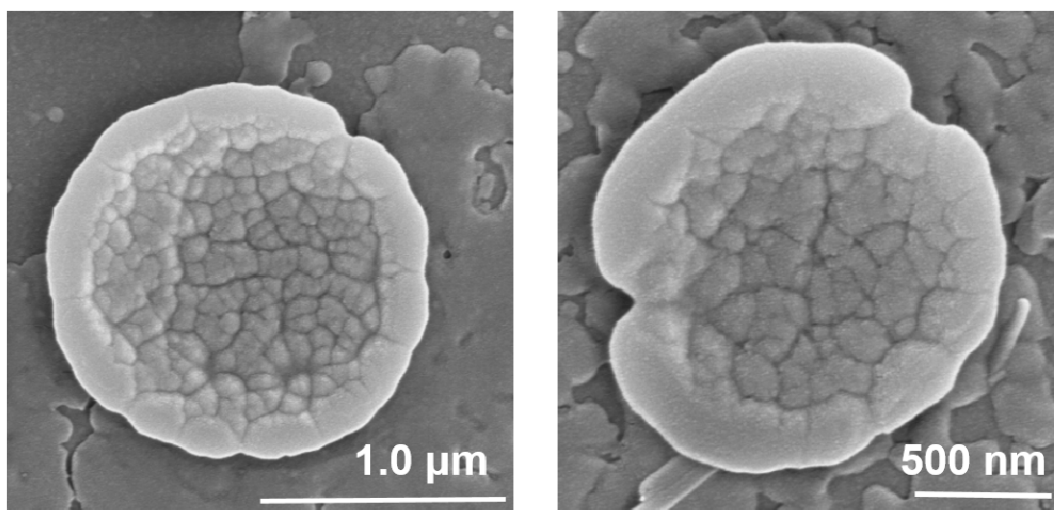**Figure S8**. SEM image of Zn−TDA (left) and Zn−TDA (right) after 20 cycles of catalysis.

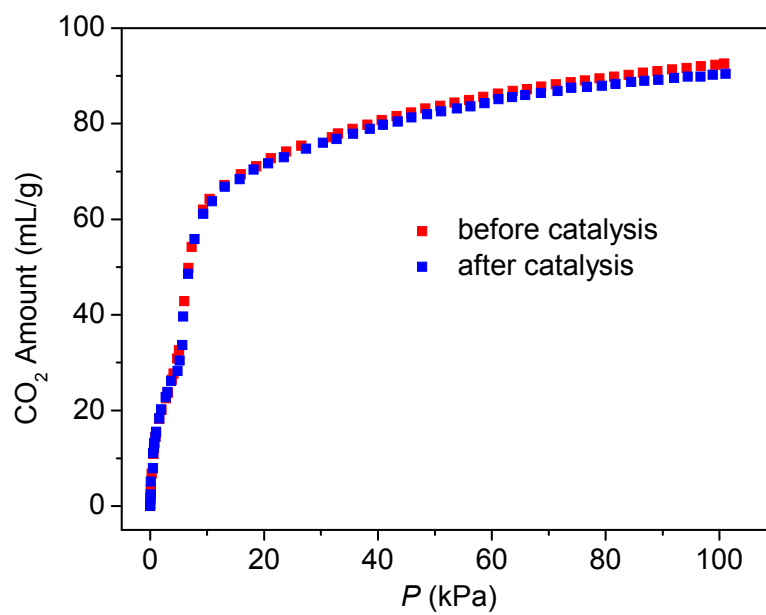**Figure S9.** CO_2 sorption isotherms of Zn−TDA before and after catalysis at 195K.

Table S2. Comparison of the isosteric heat (Q_{st}) with the selected MOFs.

Entry	MOFs	Q_{st} (kJ mol^{-1})	Ref.	Entry	MOFs	Q_{st} (kJ mol^{-1})	Ref.
1	SIFSIX-3-Zn	45	S2	12	NH$_2$-Zr(H$_2$L)	27.2	S13
2	1′	37	S3		F-NH$_2$-Zr(H$_2$L)	30.4	
3	FJI-H14	26.6-30.5	S4	13	NUC-9	25.8	S14
4	1	36.7	S5	14	Co$_7$-MOFs	25-36	S15
5	FJI-C10	20.94	S6	15	1	29	S16
6	Yb-DDPY	28.37	S7	16	1	23	S17
	Yb-DDIA	30.87			2	21	
7	1′	23.3	S8	17	MOF1′	37.1	S18
	2′	28.1		18	5a	83.3	S19
8	JLU-MOF58	19	S9	19	[Co$_2$(tzpa)(OH)]	38.5	S20
9	1a	23	S10	20	[Zn$_3$(pbdc)$_2$]·Hpip	32	S21
10	Ni-MOF-1a	33	S11	21	SNU-77H	19.4	S22
11	MOF-74-Ni	41.0	S12	22	Zn-TDA	21.7-25.2	This work

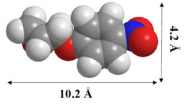# Table S3. The molecular size of selected substrates.
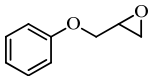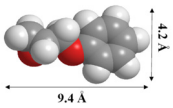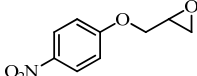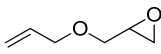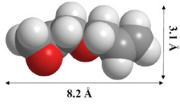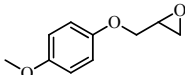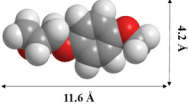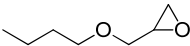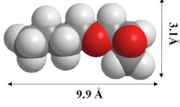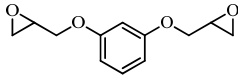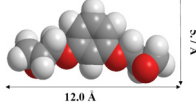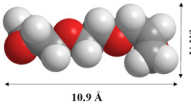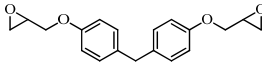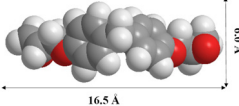
Entry	Epoxides	Molecular Size	Entry	Epoxides	Molecular Size
1		9.4 Å / 4.2 Å	5		10.2 Å / 4.2 Å
2		8.2 Å / 3.1 Å	6		11.6 Å / 4.2 Å
3		9.9 Å / 3.1 Å	7		12.0 Å / 5.7 Å
4		10.9 Å / 3.1 Å	8		16.5 Å / 6.0 Å

Table S4. Comparison with different MOFs catalysts in the cyclic addition of CO_2 and 2-(phenoxymethyl)oxirane under similar conditions (100 ℃ under 1.0 MPa CO_2).

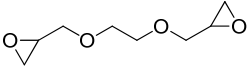| Entry	Catalyst	CO_2 uptake ($cm^3\ g^{-1}$)	Q_{st} ($kJ\ mol^{-1}$)	T (hr)	TON[a]	TOF (h^{-1})[b]	Ref.
1	Ni−TCPE1	47.8 at 273 K	-	12	2000	167	S23
		32.8 at 298 K					
2	{Ni₄L(OH)₂}	-	-	9	4000	444	S24
3	1	-	-	12	1429	119	S25
4	Zr(H₄L)	-	-	6	3000	500	S26
5	Zn-NTTA	-	-	8	3920	490	S27
	Cu-NTTA	115.6 at 273 K	-	8	3830	479	
		65.5 at 298 K					
6	1	-	-	8	25.6	3.2	S28
7	ZIF−67	-	-	14	37.3	2.7	S29
8	Zn-DPA	44.5 at 273 K	29.4–32.4	2	4000	2000	S30
		34.8 at 298 K					
9	Zn-TDA	31.4 at 273 K	21.7-25.2	1.5	10000	6667	This work
		21.5 at 298 K					

[a] TON is the turnover number: Moles of cyclic carbonate per mole of catalyst; [b] TOF is the turnover frequency: Moles of cyclic carbonate per mole of catalyst per hour.

Table S5. Comparison with different MOFs catalysts in the cyclic addition of CO_2 and 2-(phenoxymethyl)oxirane under similar conditions (r.t. under 0.1 MPa CO_2).

Entry	Catalyst	CO_2 uptake (cm^3 g^{-1})	Q_{st} (kJ mol^{-1})	T (hr)	TON[a]	TOF (h^{-1})[b]	Ref.
1	MMPF−18	60 at 273 K	23	48	133	2.8	S31
		33.6 at 298 K					
2	MMCF−2	-	-	48	300.8	6.3	S32
3	Zn-DPA	44.5 at 273 K	29.4-32.4	2	320	160	S30
		34.8 at 298 K					
4	1′	45.58 at 273 K	38.4	24	662	27.6	S33
		33.62 at 298 K					
5	1a	134.7 at 273 K	32.4	48	104.6	2.2	S34
		93.8 at 298 K					
6	JUC-1000	125 at 273 K	23	48	116	2.4	S35
		80 at 298 K					
7	PFC-31	-	-	48	71	1.5	S36
8	1	11.4 at 298 K	-	24	328	13.7	S37
9	1′	159.41 at 273 K	26.72	12	440	36.7	S38
		89.98 at 298 K					
10	1	41.75 at 298 K	32.7	24	100.4	4.2	S39
11	Zn-TDA	31.4 at 273 K	21.7-25.2	1.5	1000	667	This Work
		21.5 at 298 K					

[a] TON is the turnover number: Moles of cyclic carbonate per mole of catalyst; [b] TOF is the turnover frequency: Moles of cyclic carbonate per mole of catalyst per hour.

Supplementary Reference:

[S1] J. Wang, C. He, P. Wu, J. Wang and C. Duan, *J. Am. Chem. Soc.*, 2011, **132**, 12402–12405.

[S2] P. Nugent, Y. Belmabkhout, S. D. Burd, A. J. Cairns, R. Luebke, K. Forrest, T. Pham, S. Ma, B. Space, L. Wojtas, M. Eddaoudi and M. J. Zaworotko, *Nature*, 2013, **495**, 80–84.

[S3] A. Verma, D. De, K. Tomar and P. K. Bharadwaj, *Inorg. Chem.*, 2017, **56**, 9765–9771.

[S4] L. Liang, C. Liu, F. Jiang, Q. Chen, L. Zhang, H. Xue, H.-L. Jiang, J. Qian, D. Yuan and M. Hong, *Nature Commun.*, 2017, **8**, 1233.

[S5] P.-Z. Li, X.-J. Wang, J. Liu, H. S. Phang, Y. Li and Y. Zhao, *Chem. Mater.*, 2017, **29**, 9256–9261.

[S6] J. Liang, Y.-Q. Xie, X.-S. Wang, Q. Wang, T.-T. Liu, Y.-B. Huang and R. Cao, *Chem. Commun.*, 2018, **54**, 342–345.

[S7] N. Wei, Y. Zhang, L. Liu, Z.-B. Han and D.-Q. Yuan, *Appl. Catal. B-Environ.*, 2017, **219**, 603–610.

[S8] D. Zhao, X.-H. Liu, J.-H. Guo, H.-J. Xu, Y. Zhao, Y. Lu and W.-Y. Sun, *Inorg. Chem.*, 2018, **57**, 2695–2704.

[S9] X. Sun, J. Gu, Y. Yuan, C. Yu, J. Li, H. Shan, G. Li and Y. Liu, *Inorg. Chem.*, 2019, **58**, 7480–7487.

[S10] S. Cheng, Y. Wu, J. Jin, J. Liu, D. Wu, G. Yang and Y.-Y. Wang, *Dalton Trans.*, 2019, **48**, 7612–7618.

[S11] J. Lia, W.-J. Li, S.-C. Xu, B. Li, Y. Tang and Z.-F. Lin, *Inorg. Chem. Commun.*, 2019, **106**, 70–75.

[S12] Q. Yang, S. Vaesen, F. Ragon, A. D. Wiersum, D. Wu, A. Lago, T. Devic, C. Matineau, F. Taulelle, P. L. Llewellyn, H. Jobic, C. Zhong, C. Serre, G. D. Weireld and G. Maurin, *Angew. Chem. Int. Ed.*, 2013, **52**, 10316–10320.

[S13] X. Sun, L. Shi, H. Hu, H. Huang and T. Ma, *Adv. Sustainable Syst.*, 2020, **4**, 2000098.

[S14] H. Lv, H. Chen, L. Fan and X. Zhang, *Dalton Trans.*, 2020, **49**, 14656–14664.

[S15] Z.-X. Bian, Y.-Z. Zhang, D. Tian, X. Zhang, L.-H. Xie, M. Zhao, Y. Xie and J.-R. Li, *Cryst. Growth Des.*, 2020, **20**, 7972–7978.

[S16] M. Jia, J. Li, J. Gu, L. Zhang and Y. Liu, *Mater. Chem. Front.*, 2021, **5**, 1398–1404.

[S17] B. Zhang, P.-Y. Guo, L.-N. Ma, B. Liu, L. Hou and Y.-Y. Wang, *Inorg. Chem.*, 2020, **59**, 5231–5239.

[S18] S. S. Dhankhar and C. M. Nagaraja, *New J. Chem.*, 2020, **44**, 9090–9096.

[S19] J. Liu, M. Hang, D. Wu, J. Jin, J.-G. Cheng, G. Yang and Y.-Y. Wang, *Inorg. Chem.*, 2020, **59**, 2450–2457.

[S20] H. H. Wang, L. Hou, Y. Z. Li, C. Y. Jiang, Y. Y. Wang and Z. G. Zhu, *ACS Appl. Mater. Interfaces*, 2017, **9**, 17969–17976.

[S21] Y. Ling, M. L. Deng, Z. X. Chen, B. Xia, X. F. Liu, Y. T. Yang, Y. Zhou and L. Weng, *Chem. Commun.*, 2013, **49**, 78–80.

[S22] H. J. Park, D. W. Lim, W. S. Yang, T. R. Oh and M. P. Suh, *Chem.-Eur. J.*, 2011, **17**, 7251–7260.

[S23] Z. Zhou, C. He, J. Xiu, L. Yang and C. Duan, *J. Am. Chem. Soc.*, 2015, **137**, 15066–15069.

[S24] C.-Y. Gao, Y. Yang, J. Liu and Z.-M. Sun, *Dalton Trans.*, 2019, **48**, 1246–1250.

[S25] J. Ai, X. Min, C.-Y. Gao, H.-R. Tian, S. Dang and Z.-M. Sun, *Dalton Trans.*, 2017, **46**, 6756–6761.

[S26] C.-Y. Gao, J. Ai, H.-R. Tian, D. Wu and Z.-M. Sun, *Chem. Commun.*, 2017, **53**, 1293–1296.

[S27] X. Guo, Z. Zhou, C. Chen, J. Bai, C. He and C. Duan, *ACS Appl. Mater. Interfaces*, 2016, **8**, 31746–31756.

[S28] C. Chen, *J. Mol. Struct.*, 2020, **1208**, 127923.

[S29] B. Mousavi, S. Chaemchuen, B. Moosavi, Z. Luo, N. Gholampour and F. Verpoort, *New J. Chem.*, 2016, **40**, 5170–5176.

[S30] P. Wu, Y. Li, J.-J. Zheng, N. Hosono, K. Otake, J. Wang, Y. Liu, L. Xia, M. Jiang, S. Sakaki and S. Kitagawa, *Nature Commun.*, 2019, **10**, 4362.

[S31] W.-Y. Gao, C.-Y. Tsai, L. Wojtas, T. Thiounn, C.-C. Lin and S. Ma, *Inorg. Chem.*, 2016, **55**, 7291–7294.

[S32] W.-Y. Gao, Y. Chen, Y. Niu, K. Williams, L. Cash, P. J. Perez, L. Wojtas, J. Cai, Y.-S. Chen and S. Ma, *Angew Chem. Int. Ed.*, 2014, **53**, 2615–2619.

[S33] P. Das and S. K. Mandal, *ACS Appl. Mater. Interfaces*, 2020, **12**, 37137–37146.

[S34] X.-Y. Li, L.-N. Ma, Y. Liu, L. Hou, Y.-Y. Wang and Z. Zhu, *ACS Appl. Mater. Interfaces*, 2018, **10**, 10965–10973.

[S35] H. He, Q. Sun, W. Gao, J. A. Perman, F. Sun, G. Zhu, B. Aguila, K. Forrest, B. Space and S. Ma, *Angew Chem. Int. Ed.*, 2018, **57**, 4657–4662.

[S36] H. Xue, T. Li, Q. Yin, G. Huang and T.-F. Liu, *Chinese J. Struct. Chem.*, 2020, **39**, 2027–2032.

[S37] R. A. Agarwal, A. K. Gupta and D. De, *Cryst. Growth Des.*, 2019, **19**, 2010–2018.

[S38] V. Sharma, D. De, R. Saha, R. Das, P. K. Chattaraj and P. K. Bharadwaj, *Chem. Commun.*, 2017, **53**, 13371–13374.

[S39] V. Gupta and S. K. Mandal, *Chem. Eur. J.*, 2020, **26**, 2658–2665.